Run Group B Jeopardy Update Document

H. Avakian,[31] L. Barion,[10] M. Battaglieri,[31,12] A. Bianconi,[34,15] A.S. Biselli,[5] F. Bossù,[2] S. Boiarinov,[31] W.J. Briscoe,[8] D. Bulumulla,[25] V.D. Burkert,[31] M. Caudron,[16] L. Causse,[16] P. Chatagnon,[16] T. Chetry,[21,24] G. Ciullo,[10,6] P.L. Cole,[19,9] M. Contalbrigo,[10] A. D'Angelo,[13,27] N. Dashyan,[39] R. De Vita,[12] M. Defurne,[2] S. Diehl,[3] R. Dupré,[16] M. Ehrhart,[16,1] A. El Alaoui,[32] L. El Fassi,[21] L. Elouadrhiri,[31] A. Filippi,[14] G.P. Gilfoyle,[26] D.I. Glazier,[35] E. Golovatch,[28] R.W. Gothe,[29] Y. Gotra,[31] K.A. Griffioen,[38] L. Guo,[7] M. Hattawy,[25,1] F. Hauenstein,[25] O. Hen,[20] A. Hobart,[16] Y. Ilieva,[29] D.G. Ireland,[35] H.S. Jo,[18] K. Joo,[3] D. Keller,[37] A. Khanal,[7] H.S. Ko,[16] V. Kubarovsky,[31] L. Lanza,[13] M. Leali,[34,15] P. Lenisa,[10,6] I .J .D. MacGregor,[35] D. Marchand,[16] V. Mascagna,[33,15,*] B. McKinnon,[35] M. Mirazita,[11] A Movsisyan,[10] C. Munoz-Camacho,[16] P. Nadel-Turonski,[31] P. Naidoo,[35] S. Nanda,[21] K. Neupane,[29] S. Niccolai,[16,†] M. Osipenko,[12] L.L. Pappalardo,[10,6] K. Park,[31] E. Pasyuk,[31] O. Pogorelko,[22] K. Price,[16] B.A. Raue,[7,31] J. Ritman,[17] A. Rizzo,[13,27] F. Sabatié,[2] C. Salgado,[23] A. Schmidt,[8,20] E.P. Segarra,[20] V. Sergeyeva,[16] U. Shrestha,[24] D. Sokhan,[35] O. Soto,[11,32] N. Sparveris,[30] S. Stepanyan,[31] I.I. Strakovsky,[8] S. Strauch,[29] M. Turisini,[11] M. Ungaro,[31] L. Venturelli,[34,15] H. Voskanyan,[39] E. Voutier,[16] X. Wei,[31] L. Weinstein,[25] N. Zachariou,[36] S. Zhao,[16] and Z.W. Zhao[4,25]

(The CLAS Collaboration)

[1] *Argonne National Laboratory, Argonne, Illinois 60439*
[2] *IRFU, CEA, Université Paris-Saclay, F-91191 Gif-sur-Yvette, France*
[3] *University of Connecticut, Storrs, Connecticut 06269*
[4] *Duke University, Durham, North Carolina 27708-0305*
[5] *Fairfield University, Fairfield CT 06824*
[6] *Universita' di Ferrara , 44121 Ferrara, Italy*
[7] *Florida International University, Miami, Florida 33199*
[8] *The George Washington University, Washington, DC 20052*
[9] *Idaho State University, Pocatello, Idaho 83209*
[10] *INFN, Sezione di Ferrara, 44100 Ferrara, Italy*
[11] *INFN, Laboratori Nazionali di Frascati, 00044 Frascati, Italy*
[12] *INFN, Sezione di Genova, 16146 Genova, Italy*
[13] *INFN, Sezione di Roma Tor Vergata, 00133 Rome, Italy*
[14] *INFN, Sezione di Torino, 10125 Torino, Italy*
[15] *INFN, Sezione di Pavia, 27100 Pavia, Italy*
[16] *IJCLAB, CNRS/IN2P3, Université Paris-Saclay, 91405 Orsay, France*
[17] *Institute fur Kernphysik (Juelich), Juelich, Germany*
[18] *Kyungpook National University, Daegu 41566, Republic of Korea*
[19] *Lamar University, 4400 MLK Blvd, PO Box 10009, Beaumont, Texas 77710*
[20] *Massachusetts Institute of Technology, Cambridge, Massachusetts 02139-4307*
[21] *Mississippi State University, Mississippi State, MS 39762-5167*
[22] *National Research Centre Kurchatov Institute - ITEP, Moscow, 117259, Russia*
[23] *Norfolk State University, Norfolk, Virginia 23504*
[24] *Ohio University, Athens, Ohio 45701*
[25] *Old Dominion University, Norfolk, Virginia 23529*
[26] *University of Richmond, Richmond, Virginia 23173*
[27] *Universita' di Roma Tor Vergata, 00133 Rome Italy*
[28] *Skobeltsyn Institute of Nuclear Physics, Lomonosov Moscow State University, 119234 Moscow, Russia*
[29] *University of South Carolina, Columbia, South Carolina 29208*
[30] *Temple University, Philadelphia, PA 19122*
[31] *Thomas Jefferson National Accelerator Facility, Newport News, Virginia 23606*
[32] *Universidad Técnica Federico Santa María, Casilla 110-V Valparaíso, Chile*
[33] *Università degli Studi dell'Insubria, 22100 Como, Italy*
[34] *Università degli Studi di Brescia, 25123 Brescia, Italy*
[35] *University of Glasgow, Glasgow G12 8QQ, United Kingdom*
[36] *University of York, York YO10 5DD, United Kingdom*
[37] *University of Virginia, Charlottesville, Virginia 22901*
[38] *College of William and Mary, Williamsburg, Virginia 23187-8795*
[39] *Yerevan Physics Institute, 375036 Yerevan, Armenia*

(Dated: June 21, 2020)

I. INTRODUCTION

The CLAS12 Run Group B comprises eight experiments, 4 approved and rated by the PAC and 4 run-group proposals, sharing the same target type (liquid deuterium) and beam (11 GeV polarized electrons). They are listed in Table I.

Experiment number	Title	Contact person	PAC days (rating)
E12-07-104	Neutron magnetic form factor	G. Gilfoyle	30 (A-)
E12-09-007a	Study of parton distributions in K SIDIS	W. Armstrong	56 (A-)
E12-09-008	Boer-Mulders asymmetry in K SIDIS	M. Contalbrigo	56 (A-)
E12-11-003	Deeply virtual Compton scattering on the neutron	S. Niccolai	90 (A High Impact)
E12-09-008b	Collinear nucleon structure at twist-3 in dihadron SIDIS	M. Mirazita	RG
E12-11-003a	In medium structure functions, SRC, and the EMC effect	O. Hen	RG
E12-11-003b	Study of J/ψ photoproduction off the deuteron	Y. Ilieva	RG
E12-11-003c	Quasi-real photoproduction on deuterium	F. Hauenstein	RG

TABLE I. The eight experiments of Run Group B.

The physics objectives of Run-Group B are manifold:

- 3D nucleon structure studies (FFs, PDFs, TMDs, GPDs) using deuterium as a neutron target and measuring exclusive and semi-inclusive reactions. Main goals: access to the GPD E, leading to the contribution of quarks' angular momentum to the nucleon spin; flavor separation of GPDs and TMDs via combination of proton and deuteron observables; accurate measurement of the neutron magnetic form factor at high Q2.
- Exclusive, near-threshold coherent and incoherent J/Psi quasi-real photoproduction on deuteron, to study the gluonic structure of bound nucleons and the deuteron, and search for isospin partners of the LHCb pentaquark.
- In-medium structure functions, Short Range Correlations, and the EMC effect, studied via proton-DIS with neutron-spectator tagging, to be compared to free-proton DIS results.
- Quasi-real $p\bar{p}$ photoproduction to look for $p\bar{p}$ resonances and study the coherent production mechanism on deuterium

The beam time allocated for Run-Group B is 90 PAC days, corresponding to the time assigned to the nDVCS experiment. The nDVCS experiment was labeled as High Impact by PAC 41, with the motivation that "once the scaling for Deep Exclusive Scattering is established, the highest goal of the GPD program is understanding of the nucleon's angular momentum carried by quarks, through the measurement of the nucleon helicity-flip GPD (E)." (PAC41 report). Run-Group B has so far obtained 39 out of the 90 awarded PAC days. In order to optimize the science impact of JLab, allocating the remaining time is essential to reach the necessary accuracy to extract E on a vast phase space.

II. EXPERIMENTAL SETUP

Run-group B uses the CLAS12 spectrometer in its baseline configuration, plus the Forward Tagger (FT), the RICH, and the Central Neutron Detector (CND, Fig. 1), which were all already installed and commissioned before the first CLAS12 experiment (RG-A). In addition, the Backward Angles Neutron Detector (BAND) was installed right before the beginning of the experiment. The CLAS12 cryogenic target (5-cm long), filled with liquid deuterium (D2) at 23 K, is used.

A. Performance of the CND

The CND was conceived to provide neutron detection efficiency in the Central Detector for the nDVCS experiment. The neutrons from nDVCS, for beam energies of about 11 GeV, are in fact expected to be emitted mainly at angles

* Current address:Università degli Studi di Brescia, 25123 Brescia, Italy
† Contact person: silvia@jlab.org

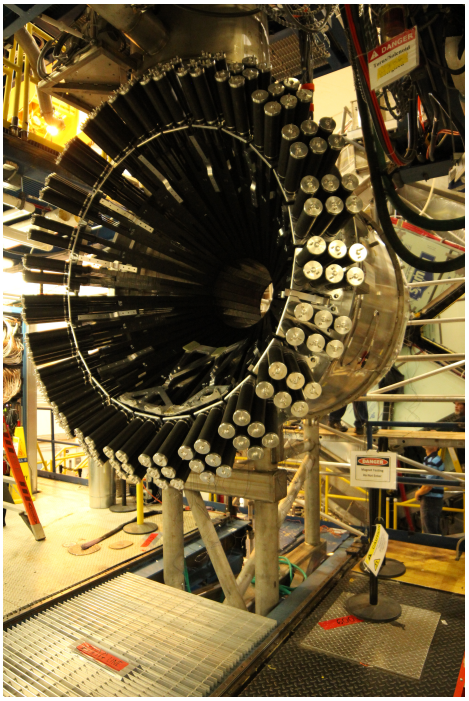

FIG. 1. The Central Neutron Detector for CLAS12, right after its installation in the CLAS12 solenoid.

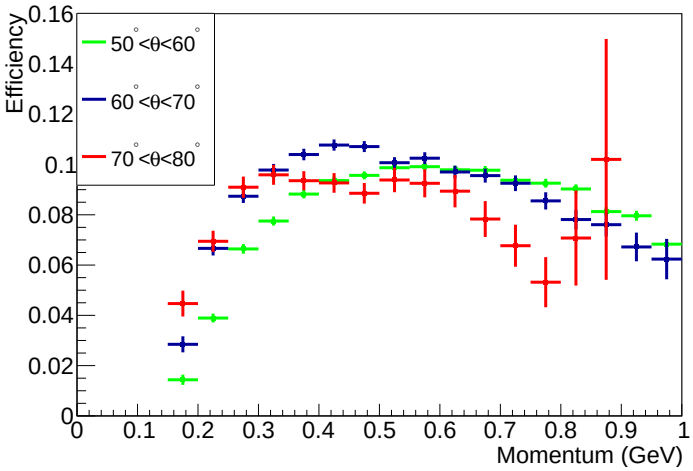

FIG. 2. Neutron detection efficiency of the CND, measured with CLAS12-RGA data.

above 40°, where the baseline CLAS12 setup had no neutron detector. The CND was installed and commissioned in the fall of 2017, and has been running since. The data taken on a proton target during the RG-A period were used to develop calibration procedures and to estimate the performances of the CND. Figure 2 shows the neutron detection efficiency measured from the the $ep \rightarrow e'n\pi^+$ channel. The data used were taken, during RG-A, with a 7.5-GeV electron beam incident on a liquid-hydrogen target. Events with an electron and a π^+ in the CLAS12 Forward Detector were selected. The missing particle was required to be in the CLAS12 Central Detector ($\theta > 40°$). From this set of $ep \rightarrow e'(n)\pi^+$ events, events with a neutron identified by the CND (CND cluster with $E_{dep} > 2.5$ MeV, no associated CVT tracks, $\beta < 0.8$) were selected. The efficiency was measured in bins of missing neutron polar angle and as a function of missing momentum. For each bin in polar angle and momentum, the efficiency is defined as the ratio of events with a detected neutron to the number of missing neutron events. The result is shown in Fig. 2. The detection efficiency extracted from this method is consistent with simulation predictions and with the design specifications of the CND.

B. Performance of BAND

The tagged deep inelastic scattering measurements require the detection of backward-angle recoil neutrons with momenta above 200 MeV/c. BAND [1] is designed to measure these neutrons at angles from 155° to 175°, with an average detection efficiency of 35%, and with a momentum reconstruction resolution better than 1.5%. The detector consists of scintillator bars with PMT readout on both bar ends. BAND was installed in January 2019 and has taken data in coincidence with CLAS12 during RG-B. Fig. 3 shows the upstream side of BAND in Hall B during installation.

Neutrons in BAND are identified in the $d(e, e')X$, data by cutting on the time-of-flight per pathlength (ToF/m), where ToF is the time difference between the time that the electron interacted in the target and the particle arrival time measured by BAND (see Fig. 4 for data with a minimum energy deposition cut of 5 MeV). There are well-separated peaks for photons and for neutrons on top of a flat background from accidental coincidences. The minimum energy deposition cut for neutron-signals will be optimized during the analysis by maximizing the neutron signal-to-background ratio and minimizing the experimental uncertainties.

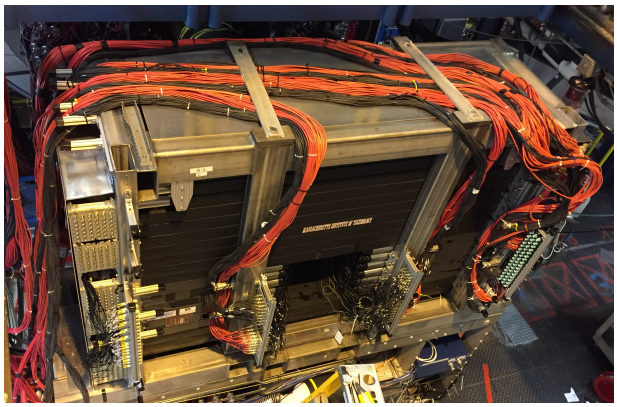

FIG. 3. BAND in Hall B. Upstream side with first set of cables installed. Picture taken from [1].

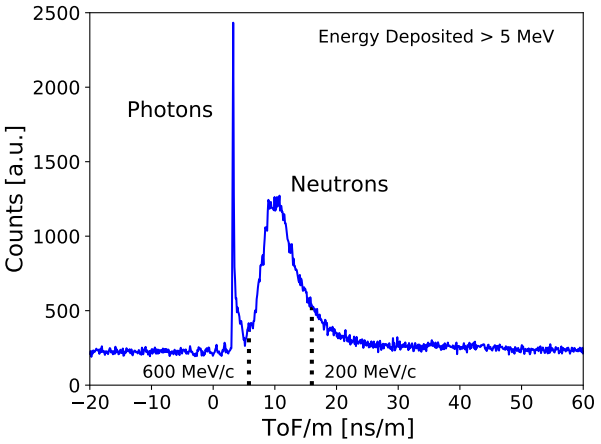

FIG. 4. Time-of-flight per meter of BAND hits in coincidence with electrons measured with RG-B data. A sharp photon peak and a broad neutron peak are visible over a flat background from accidentals. The dashed lines indicate the range of neutrons with momenta between 200 and 600 MeV/c. Picture taken from [1].

III. OVERVIEW OF THE THREE RUN PERIODS

RG-B has run during three periods of roughly one calendar month each, between the end of winter 2019 and the beginning of 2020, for a total of about 38.9 PAC days. The average beam polarization was about 85%, with variations of a couple of percent during the different run periods.

A. Spring 2019

The experiment ran from February 8 to March 25 2019. The first half had a beam energy of 10.6 GeV, which was subsequently lowered to 10.2 GeV, from March 8 onwards, due to accelerator problems. From the beam-time accounting of CEBAF:

- Available Beam in Use (ABU): 522.8 hours
- Beam Available but Not Used (BANU): 79.1 hours
- Beam Not Available (BNA): 374.6 hours.

Thus, this run achieved a total of 21.7 PAC days according to ABU. Roughly 9.7 B triggers at 10.6 GeV and 11.7 B at 10.2 GeV were collected, with the CLAS12 torus in inbending configuration.

B. Fall 2019

The experiment ran from December 3 to December 20 2019. The beam energy was, this time, 10.4 GeV. From the beam-time accounting of CEBAF:

- ABU: 161.6 hours
- BANU: 36 hours
- BNA: 184.8 hours.

This run corresponded to 6.7 PAC days according to ABU. Roughly 9.0 B triggers were collected, with the CLAS12 torus in outbending configuration.

C. Winter 2020

The experiment ran from January 7 to January 29 2019. The beam energy was 10.4 GeV. From the beam-time accounting of CEBAF:

- ABU: 244.7 hours
- BANU: 35.2 hours
- BNA: 281.3 hours.

This run corresponded to 10.5 PAC days according to ABU. Roughly 12.9 B triggers were collected, with the CLAS12 torus in inbending configuration.

IV. PRELIMINARY RESULTS

A. Neutron Magnetic Form Factor G_m^n

The elastic electromagnetic form factors are basic observables that describe the distribution of charge and magnetization inside the proton and neutron. Their measurement is a goal of the current NSAC Long-Range Plan and it forms a central part of the physics programs at JLab. We are part of a broad campaign to measure the four elastic, electromagnetic, nucleon form factors (electric and magnetic ones each for the proton and neutron) at JLab that includes seven experiments approved for running during the 12 GeV era.

We are using the ratio of $e-n$ to $e-p$ events in quasi-elastic (QE) kinematics to extract G_M^n. This ratio method is less sensitive to experimental parameters like luminosity, electron reconstruction efficiency, trigger efficiency, *etc.* We then use the better known proton magnetic and electric form factors (G_M^p and G_E^p) along with the small contribution of the neutron electric form factor (G_E^n) to determine G_M^n. With CLAS12 we apply acceptance matching in constructing the ratio. We use the measured, scattered electron information and, assuming QE kinematics, calculate both proton and neutron trajectories through CLAS12. If both calculated trajectories strike the detector fiducial volume we keep the event. This method ensures the acceptance for neutrons and protons overlaps. We have developed and tested computer codes written with the CLAS Common Tools (COATJAVA) in simulation and are now applying them to the early passes of the Run Group B deuteron data. Figure 5 shows the impact in simulation of switching on acceptance matching and applying a cut on the direction of the outgoing detected proton requiring it to be close to the direction of the virtual photon. This angle cut preferentially selects QE events. The sequence shows how we can separate the QE events from other, inelastic ones.

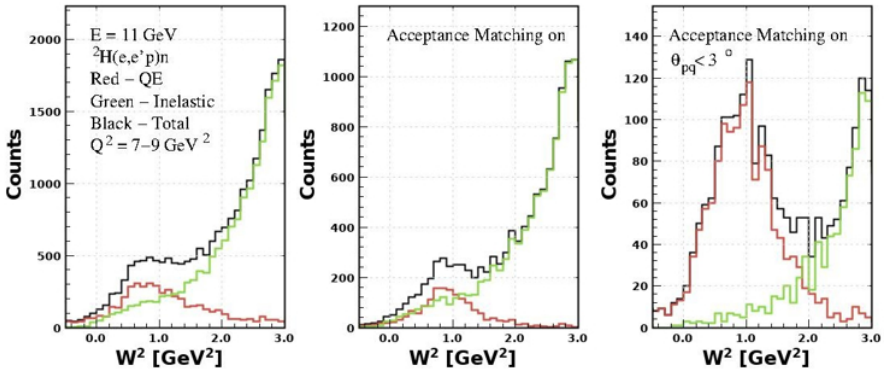

FIG. 5. Simulation of the W^2 distribution for $e-p$ events with different kinematic cuts. The angle θ_{pq} is between the transferred 3-momentum and the proton momentum.

A crucial step in extracting the $e-n/e-p$ ratio is to measure the neutron detection efficiency (NDE) for the Forward Detector of CLAS12 to accurately determine the numerator. To that end we are using the ^{1}H(e, e$'\pi^+$n) reaction on a hydrogen target as a source of tagged neutrons. We measure the missing 4-momentum from ^{1}H(e, e$'\pi^+$), extract the square of the missing mass MM^2, and apply a cut around the neutron MM^2. We use the missing 3-momentum in the reaction to predict where the neutron should be detected in CLAS12 and then require a neutron to appear in

a narrow cone around that direction. We are using Run Group A and K data to extract the NDE. Very preliminary results are shown in Figure 6. The left-hand panel shows the final MM^2 distribution for neutral particles from the Run Group A data. We see clear separation of the photons and the neutrons. The right-hand panel shows the preliminary NDE (red) compared with the previous measurement of the NDE in the CLAS6 G_M^n measurement. We continue to optimize these results and investigate other data sets (Run Group K) to study the systematic behavior of the NDE.

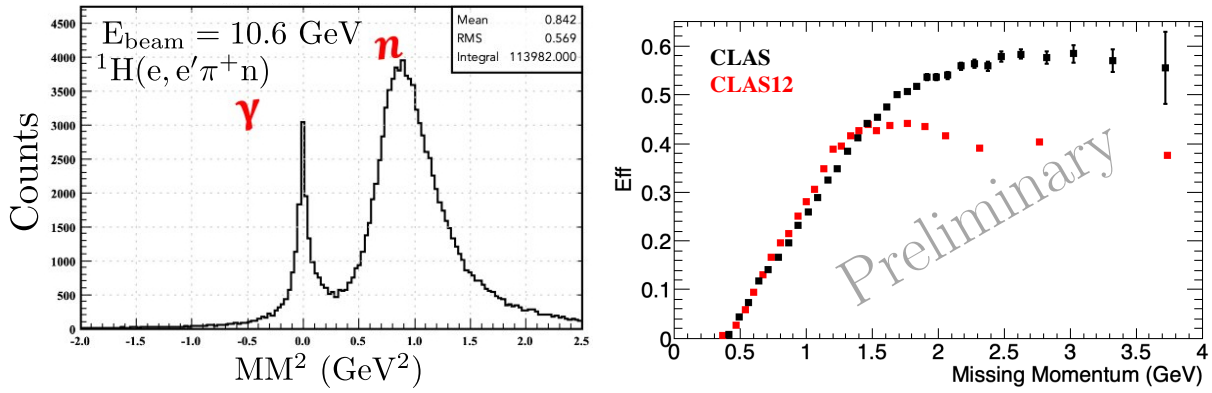

FIG. 6. MM^2 distribution (left-hand panel) for NDE calibration reaction and the preliminary NDE (red) versus neutron momentum (right-hand panel) in the EC/PCAL in the Forward Detector. The black points are from the CLAS6 G_M^n measurement.

In the last year we have formed a group with Dr. Brian Raue at Florida International University and his doctoral student Lamya Baashen. The G_M^n analysis will be her thesis project.

B. nDVCS

Measuring Deeply Virtual Compton Scattering on a neutron target is one of the necessary steps to complete our understanding of the structure of the nucleon in terms of Generalized Parton Distributions (GPDs). DVCS on a neutron target allows to operate a flavor decomposition of the GPDs and plays a complementary role to DVCS on a transversely polarized proton target in the determination of the GPD E, the least known and least constrained GPD that enters Ji's angular momentum sum rule [2].

The importance of neutron targets in the DVCS phenomenology was clearly established in the pioneering Hall A experiment, where the polarized-beam cross section difference off a neutron, from a deuterium target, was measured [3]. This experiment was recently followed by a second, higher-statistics, analysis of 6-GeV Hall A [4] data on deuterium target. This analysis leads to a model-dependent extraction of three combinations of Compton Form Factors (CFFs, which are integrals of GPDs) separated into quark flavors, via a measurement of the nDVCS cross section at two different beam energies. One of the limits of both Hall-A nDVCS experiments is the lack of exclusivity: only the electron and the photon are detected, and the $en\gamma$ yield is obtained by subtracting proton target data from deuteron target data, and removing the background from coherent deuteron DVCS with a missing-mass selection cut. While the semi-inclusive detection topology ($e\gamma X$) allows to achieve a high statistical accuracy, sizeable systematic uncertainties remain due to the subtraction procedures. Moreover, the kinematics reach of the Hall-A experiments was limited by the low electron beam energy.

Our experiment aims to perform, for the first time, a fully exclusive extraction of the neutron-DVCS reaction by detecting the recoiling neutron. It will measure, over a wide phase space, the beam-spin asymmetry (BSA), which has a direct sensitivity to E, the least known and constrained GPD. Furthermore, the high energy electrons of the upgraded CEBAF permits to cover unexplored kinematics, in particular the low-x_B region, where models, such as VGG [5], predict the BSA to be sizeable, and high Q^2, where the leading-twist GPD formalism can be applied.

A preliminary raw beam-spin asymmetry for nDVCS was extracted from a subset of the spring RG-B data, which were calibrated and reconstructed before the DNP-2019 fall meeting. These data, which correspond to roughly 25% of the spring dataset, are referred to as "DNP data", and are used for all results shown in this report. $ed \to en\gamma(p)$ events were selected applying particle identification followed by a set of stringent exclusivity cuts. The left plot of Fig. 7 shows the missing mass of the $en \to en\gamma X$ system after the application of all exclusivity cuts. The resulting beam-spin asymmetry is displayed in the right plot of Fig. 7, and fitted with the $a \sin\phi$ function. Although this is a raw asymmetry (without background subtraction), obtained with a small fraction of the data and after only preliminary calibrations, the shape and size of the asymmetry are compatible with expectations. Work is ongoing to

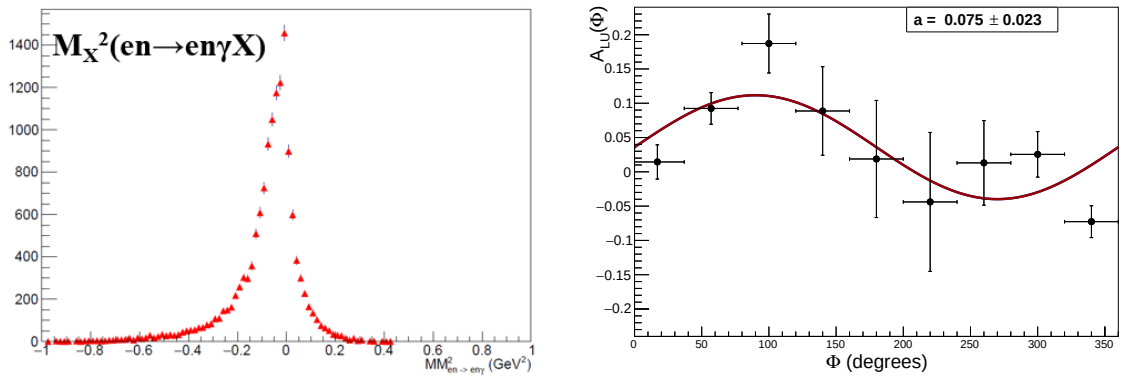

FIG. 7. Left: Mass of X in the $en \to en\gamma X$ reaction, after application of all other exclusivity cuts. Right: Raw beam-spin asymmetry for the DVCS on the neutron, obtained using the "DNP data", as a function of ϕ and integrated over all other kinematic variables.

estimate the neutral pion contamination in the $en\gamma$ event sample.

The result shown in Fig. 7 is obtained combining runs taken with 10.6 and 10.2 GeV beam energy. While this is acceptable for a rough, preliminary result, combining BSAs obtained with different beam energies is a complex operation, due to the strong beam-energy dependence of the Bethe-Heitler cross section. Depending on the kinematics, and especially at the edges of the ϕ distribution, the nDVCS/BH cross section can vary strongly following a variation of 400 MeV in the beam energy. Although the BSA is less sensitive than the cross section to the beam energy (as the BSA is proportional to the DVCS/BH interference term), the steep variation of the cross section affects the value of the central kinematics for each bin, making the combination of the asymmetries a not-straightforward task, requiring model-dependent corrections. The combination of the three datasets, therefore, will induce model-dependent systematic uncertainties. It will be crucial to have a stable, high-statistics run, possibly at one of the beam energies already used, for the remainder of the data taking.

C. SIDIS di-hadron production

In the di-hadron SIDIS production, two hadrons are detected in the final state together with the scattered electron. The goal of the experiment is a comprehensive investigation of the nucleon structure through the study of several observables in the collinear approximation, i.e. when the transverse momenta of the final particles are integrated out. In this limit, the di-hadron cross section can be written as a product of a nucleon PDF (which depends on x_B) and a di-hadron Fragmentation Function (DiFF), which depends on the invariant mass of the hadrom pair M_h and their total energy fraction z. In addition, both the PDF and the DiFF depends on Q^2 through the evolution equation.

The two reference measurements of the experiment are the multiplicity and the Beam Spin Asymmetry (BSA). A combined analysis of the data on proton (from the RG-A run period) and deuteron data will allow to perform the flavor separation of the observables of interest. As a representative example of the ongoing analysis, we concentrate in the following on the multiplicity analysis in the $e\pi^+\pi^- X$ final state. Parallel analysis for other pion pair charge combinations are also being performed on both multiplicity and BSA.

The multiplicity is defined as the ratio between the di-hadron cross section and the inclusive DIS cross section:

$$M(x_B, z, M_h; Q^2) = \frac{\frac{d\sigma^{dh}}{dx_B dz dM_h dQ^2}}{\frac{d\sigma^{DIS}}{dx_B dQ^2}} \tag{1}$$

where, up to various kinematical factors, the di-hadron cross section can be written as a a sum over the quark flavors q

$$d\sigma^{dh} \propto \sum_q e_q^2 f_{1,q}(x_B) D_{1,q}(z, M_h) \tag{2}$$

with $f_{1,q}$ being the well known unpolarized PDFs and $D_{1,q}$ the, basically unknown, unpolarized DiFFs. It is easy to see that the uncertainty in the extraction of the $D_{1,u}$ from the data is largely dominated by the uncertainty on the

proton multiplicity, while the uncertainty on the deuteron multiplicity plays a crucial role in the extraction of the $D_{1,d}$.

From the experimental point of view, the multiplicities are computed as the ratio of the acceptance corrected number of di-hadron events to the number of inclusive electrons. We show here the preliminary results of the analysis performed on the DNP-2019 cooking, which includes about 30% of the RG-A Fall 2018 data (corresponding to few percent of the whole data set) and about 25% of the RG-B Spring 2019 data (∼10% of the whole dataset). A number of kinematic cuts has been applied to select the DIS regime and pions produced in the current fragmentation region, namely: $Q^2 > 1$ GeV^2, $W > 2$ GeV, $x_F > 1$. In addition, the cut $y < 0.85$ is applied to suppress rediative events. Finally, a cut on the missing mass $MM(e\pi^+\pi^-X)$ >1.1 GeV has been applied in order to remove exclusive $ep\pi^+\pi^-$ events.

The Monte Carlo simulations are performed using the CLAS-DIS event generator and the gemc CLAS12 response simulations. The reconstruction and the analysis of the simulated data is performed using the same code as for the experimental data.

The preliminary results are presented in a fully unintegrated 4D grid, with three Q^2 bins, eight bins in z and M_h and six bins in X_B, for a total of more than thousand independent bins (but many of the edge bins are empty to the available phase space a the CLAS12 energies). An example of the quality of the data is shown in Fig. 8. Here we selected one bin in x_B and z and we plotted the multiplicity as a function of the M_h for 3 bins in Q^2. The black points represent the results on the proton data, while the red points the results for the deuteron target. The error bars in the plots include the statistical uncertainty on both the experimental events and the Monte Carlo acceptance. The vertical red dashed line indicates the position of the ρ mass.

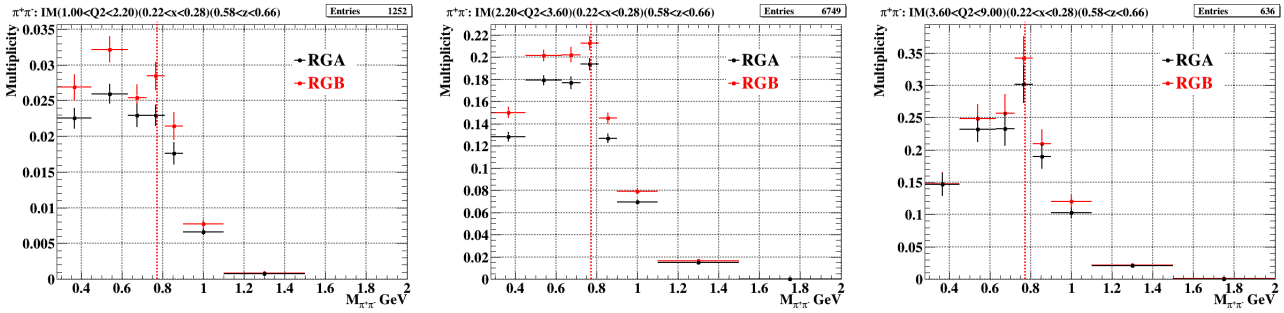

FIG. 8. Di-hadron multiplicity as a function of M_h from DNP-2019 data on the proton (black points) and deuteron (red points) target. The plots refer to the bin $0.22 < x_B < 0.28$, $0.58 < z < 0.66$ and, from left to right: $1 < Q^2 < 2.2$ GeV^2, $2.2 < Q^2 < 3.6$ GeV^2 and $3.6 < Q^2 < 9.0$ GeV^2. The vertical dashed lines indicate the position of the ρ mass.

We see that the statistical error of the two data sets is comparable in the plots shown, and the same happens for basically all the kinematic bins. On the other hand, the error bars are sufficiently small for a reliable extraction of the DiFF only where the bulk of the statistics is concentrated, i.e. at low Q^2, central values of z and x_B (as in the bins shown n Fig. 8) and low invariant mass. Therefore, the completion of the data taking on both proton and deuteron targets will be crucial for the accurate determination of the multiplicity over the whole kinematic plane. The benefit of about one order of magnitude higher statistics than what is shown in the Figs. 8 on both targets will be definitely more important for the other combination of pion charge, which are also under analysis.

D. Tagged DIS measurements with BAND

Tagged deep inelastic scattering measurements of spectator neutrons allows the study of the bound proton structure function F_2^{*p} when that proton is in a high-momentum, highly-virtual state. We will extract the ratio of bound to free structure function as a function of spectator neutron light-cone momentum fraction α_s by measuring ratios of high-x' to low-x' $d(e,e'n)X$ events (x' is the Bjorken scaling variable for a moving nucleon). Comparing the ratio with theoretical predictions allows one to disentangle the various effects (nucleon motion, short-range correlations, binding) to the modification of the structure function.

The analysis status presented here is based on the "DNP data" (see previous section) which corresponds to about 25% of the RG-B spring 19 data. For the $d(e,e'n)X$ events, we select electrons based on standard CLAS12 PID and fiducial cuts and a $W > 2$ GeV cut to select DIS events. The neutrons are selected based on the ToF/m spectrum of their hits in BAND. In general, the neutrons have momenta between 200 MeV/c and 600 MeV/c.

The data is binned in Q^2, θ_{nq}, x' and α_s. The kinematic dependencies of the variables do not allow for a simple subtraction of accidental background events which are present in the neutron peak in the BAND time of flight spectrum (see Figure 4). We developed a procedure based on event-mixing to determine the shape and amount of background in each of our bins. First, we store the information about the electrons and neutrons in separate files. Afterwards, we combine every neutron randomly with 100 electrons to create an event-mixed background file.

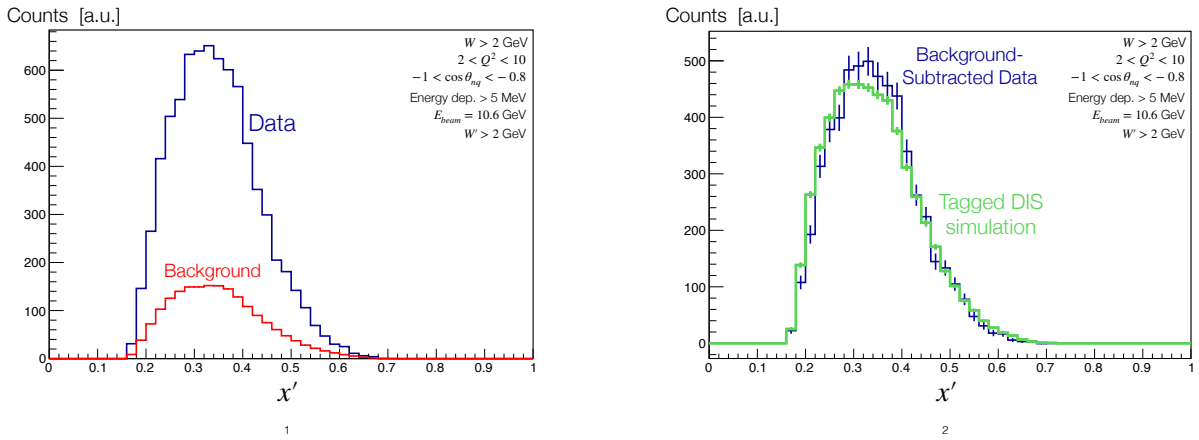

FIG. 9. (left) x' distribution for $d(e,e'n)X$ events at 10.6 GeV beam energy with data shown in blue and background from event-mixing shown in red. (right) x' distribution from data with background subtracted (black) and from simulations (green).

Figure 9 (left) shows the x' distribution for $d(e,e'n)X$ events at 10.6 GeV beam energy (blue) and the background from the event-mixing procedure (red). The data is shown for the bin $[2 < Q^2 < 10, -1 < \cos(\theta_{nq}) < -0.8]$ and an additional cut $W' > 2$ GeV. As one can see, the data reaches x' values up to 0.55. In Figure 9 (right) the background subtracted x' distribution (black) is compared with results from simulations (green). The overall good agreement shows that our background subtraction works. A first set of results based on the spring 2019 data is expected next year.

E. J/ψ Photoproduction off Deuteron

The objective of this scientific program is to measure the differential cross section of (a) the incoherent, (b) the coherent production of J/ψ meson off the deuteron, and (c) the cross section of J/ψ production off the neutron. The program aims to address several interesting physics aspects of the J/ψ production dynamics that cannot be answered by measurements off a proton target. The RGB experiment provides the very first measurement of exclusive J/ψ photoproduction off deuteron from threshold up to 11 GeV and at $Q^2 = 0 - 0.02$ $(\mathrm{GeV}/c)^2$. By accessing directly the $J/\psi N$ elastic scattering in final-state interactions, we aim to assess the largely unknown low-energy total $J/\psi N$ cross section; by measuring the unexplored quasi-free (QF) J/ψ photoproduction off the neutron, we aim to provide evidence for (or against) a pentaquark decaying into $J/\psi n$; the measurement of the coherent process at large momentum transfer would provide a first glimpse into the nuclear gluon distribution a decade before the advent of the Electron-Ion Collider (EIC).

The J/ψ proposal joined RGB in 2018 and the relevance and the significance of all three components of the measurement continue to be high. The nuclear aspect of the program remains unique as there are no other competing data or expected exclusive experiments on deuteron or light nuclear targets. Despite the recently published cross section of J/ψ real photoproduction off the proton by the GlueX Collaboration, the question whether there is a charmed pentaquark signal in near-threshold photoproduction of J/ψ off the neutron is still valid and will remain valid independent of whether the recent measurements of J/ψ off the proton in Hall B (RGA) and/or Hall C observe a pentaquark signal.

The reactions $\gamma d \to J/\psi pn$ and $\gamma d \to J/\psi d$ are being measured in untagged quasi-real photoproduction, where all the final state particles (the nucleon(s) or deuteron, and the lepton pair from the J/ψ decay) are detected so that the photon is reconstructed via 4-momentum conservation.

Due to the small cross section of near-threshold J/ψ photoproduction, the quality of detector calibrations and the availability of a large sample of calibrated data are critical to demonstrate the viability of the experimental method.

Since none of these conditions are satisfied by the "DNP data", here we provide a very preliminary e^+e^- invariant mass distribution (Fig. 10) to show the current status of the data analysis. The two leptons are identified by constraining the energy deposition in the electromagnetic calorimeters and the number of photoelectrons in the High-Threshold Cherenkov Detector. Additionally, the momenta and the scattering angles of the leptons are constrained according to the J/ψ decay kinematics. Events with small opening angle between the two leptons are suppressed by excluding pairs detected in the same, or in neighboring, sectors. Due to the limited amount of data, no exclusivity cuts have been applied. One can see small enhancements at the locations of ρ/ω, ϕ, and J/ψ, which is encouraging. Further methods for background studies and reduction will be developed during the rest of this year, especially when the rest of the data sample becomes available for physics analysis.

The remaining beam time for this program is critical in order to be able to deliver statistically significant cross sections for the three physics topics of interest.

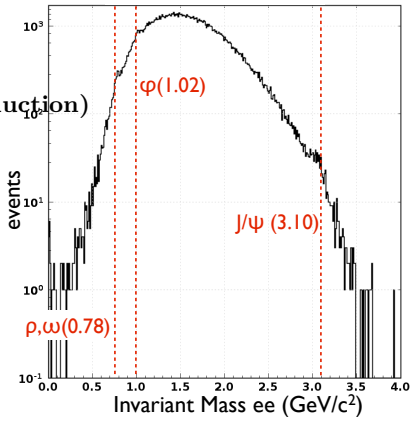

FIG. 10. Electron-Positron invariant-mass distribution for the $ed \to e^+e^-X$ reaction.

F. New analyses (pDVCS, dDVCS, π^0-production)

In addition to the original proposals, the RG-B data are being analyzed for new first-time measurements.

The coherent deuteron DVCS, $eD \to eD\gamma$, provides access to deuteron GPDs. The deuteron has spin 1 and it has a rich structure described by nine GPDs which are completely unknown as of today. The beam spin asymmetry depends on three of these nine GPDs and it is expected to have a $\sin\phi$ dependence. The data are analyzed requiring a a fully exclusive final channel, and tight kinematic cuts are imposed to ensure the exclusivity. The electron is detected in the FD, the photon in both the FT and FD, while the deuterons are found in the CD. The statistical accuracy is limited but the analysis is showing a promising 10-20% raw beam spin asymmetry, as displayed in Figure 11.

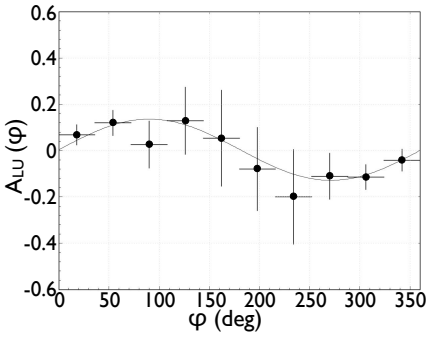

FIG. 11. BSA for the coherent deuteron DVCS.

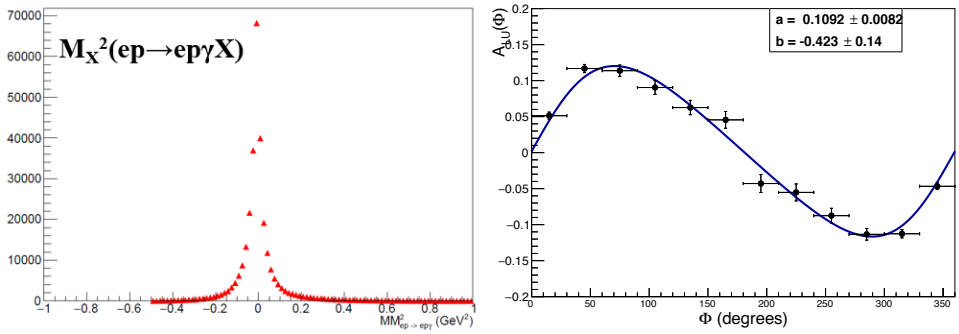

FIG. 12. Left: Mass of X in the $ep \to e\gamma X$ reaction, after application of all other exclusivity cuts. Right: BSA for the incoherent proton DVCS on a deuterium target.

An analysis is also ongoing to extract incoherent proton DVCS on a deuterium target. The interest for this channel is twofold:

- to understand nuclear-medium effects on GPDs, along the line of the experiments being carried out at CLAS on He^4 [6]
- a comparison between free-proton pDVCS and incoherent pDVCS on deuterium will help extract the free-neutron nDVCS from the incoherent one.

Complementary to the physics goals of DVCS measurements, hard exclusive production of mesons allows access to the so-called "transversity" GPDs. Pseudoscalar exclusive electroproduction has been found to be particularly sensitive to transversity GPDs [7, 8]. Analysis is in progress to measure, for the first time, the BSA of exclusive π_0-production from the neutron. Aside from its intrinsic interest, this process is also a source of background for the $en\gamma$ final state, and a measure of its asymmetry is a necessary step to extract the nDVCS beam-spin asymmetry from

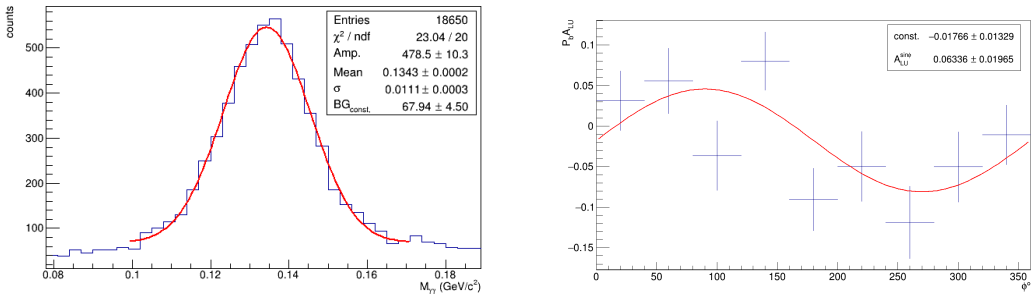

FIG. 13. Left: Invariant mass of photon pairs from all detector combinations for exclusive $ep \to e'p'\gamma\gamma$ events, showing a peak at the π_0 mass. Right: Preliminary Beam Spin Asymmetry for π_0-production on the proton in deuterium, scaled by the beam polarisation, P_b.

the raw one. The analysis procedure was initially developed on the proton in the deuteron. Results for the neutron are as yet unavailable, but a preliminary BSA in π^0-production from the proton can be seen in figure 13. Work is ongoing on the optimisation of the channel selection.

V. CONCLUSIONS

Run-group B, which primarily aims to investigate the partonic structure of the neutron and to ultimately achieve, in combination with proton-target experiments, flavor separation of various multi-dimensional structure functions, has run during part of the year 2019, collecting 38.9 PAC days, and with three different electron beam energies. Preliminary analyses on a subset of roughly 10% of the data taken so far show promising results for some the originally proposed measurements as well as for new reaction channels. More statistics is needed in order to be able to sample the multi-dimensional kinematic dependence of the measured observables. For nDVCS, in particular, it is also crucial to be able to collect data with a single value of beam energy. We request the PAC to confirm, for RG-B, the original approved beamtime for the nDVCS experiment (90 days), awarding us therefore 51 more PAC days of running.

REFERENCES

[1] E.P. Segarra et al. The CLAS12 Backward Angle Neutron Detector (BAND). 2020.
[2] Xiang-Dong Ji. Gauge-Invariant Decomposition of Nucleon Spin. *Phys. Rev. Lett.*, 78:610–613, 1997.
[3] M. Mazouz et al. Deeply virtual compton scattering off the neutron. *Phys. Rev. Lett.*, 99:242501, 2007.
[4] M. Benali et al. Deeply virtual Compton scattering off the neutron. *Nature Phys.*, 16(2):191–198, 2020.
[5] M. Vanderhaeghen, Pierre A.M. Guichon, and M. Guidal. Deeply virtual electroproduction of photons and mesons on the nucleon: Leading order amplitudes and power corrections. *Phys. Rev. D*, 60:094017, 1999.
[6] M. Hattawy et al. Exploring the Structure of the Bound Proton with Deeply Virtual Compton Scattering. *Phys. Rev. Lett.*, 123(3):032502, 2019.
[7] I. Bedlinskiy et al. Measurement of Exclusive π^0 Electroproduction Structure Functions and their Relationship to Transversity GPDs. *Phys. Rev. Lett.*, 109:112001, 2012.
[8] I. Bedlinskiy et al. Exclusive π^0 electroproduction at $W > 2$ GeV with CLAS. *Phys. Rev. C*, 90(2):025205, 2014. [Addendum: Phys.Rev.C 90, 039901 (2014)].